



Research paper

A pharmacokinetic study of a combination of beta adrenoreceptor antagonists – In the isolated perfused ovine eye

Jenifer Mains, Lay Ean Tan, Clive Wilson, Andrew Urquhart*

Strathclyde Institute of Pharmacy and Biomedical Sciences, University of Strathclyde, Scotland, United Kingdom

ARTICLE INFO

Article history:

Received 10 June 2011

Accepted in revised form 10 November 2011

Available online 20 November 2011

Keywords:

Ocular

Pharmacokinetics

Mass spectrometry

Isolated perfused

Beta adrenoreceptor antagonist

ABSTRACT

The treatment of posterior eye diseases, such as diabetic retinopathy and age-related macular degeneration, is of growing interest as the number of people affected by these conditions continues to rise. This study utilises the methods of cassette dosing and the perfused ovine eye model – to reduce animal usage and therefore animal time – to show that for a series of beta adrenoreceptor antagonists, lipophilicity is a key physicochemical property that governs drug distribution within the eye. Following intravitreal injection, lipophilic beta adrenoreceptor antagonists penetrate to the posterior eye, where they bind to the choroid and reside in the retina at greater concentrations than more hydrophilic beta adrenoreceptor antagonists, which preferentially penetrate to the anterior eye.

© 2011 Elsevier B.V. All rights reserved.

1. Introduction

Interest in drug disposition in posterior eye disease has increased in recent years especially when treating certain disease states – such as diabetic retinopathy and age-related macular degeneration – where effective treatment is currently limited. Understanding the factors that influence drug disposition can potentially improve treatment options in these conditions by enabling improved drug targeting to the desired site of action and prediction of toxicity problems. The difficulty with describing ocular drug disposition mainly arises from the fact that it is not just a matter of taking a simple blood sample from the specimen at various time points and creating a concentration versus time profile although, in the fluid based ocular structures, namely the aqueous and vitreous humour, it is possible to sample a very small volume of fluid without the need for total eye enucleation. However, this technique cannot be applied to the remaining tissues present in the eye. For this reason, an animal is required for each time point, and repeat experiments are necessary. Therefore, in order to obtain information regarding the movement of substances within the eye, many animals are required to cover a significant time range, and each tissue has to be subjected to analysis individually. This leads to large animal requirements, prolonged analytical time and also the problem of inter-animal variability. In an attempt to overcome these problems, cassette dosing can be used. Cassette dosing

involves administering a series of drug compounds to the animal simultaneously in one dose, the 'cassette'. Commonly, a small cassette is used of approximately 2–10 compounds, at a low dose of up to about 1 mg/kg/compound for systemic studies [1,2]. The benefits of cassette dosing include reduced animal usage and reduced animal variability along with reduced analytical time, especially during the method development process. One major issue regarding cassette dosing is the potential for drug interactions between the drugs contained in the cassette. Possible sources of interaction are competition for clearance pathways, competition for protein binding, activation of certain clearance pathways, effects on blood flow and enzyme induction, solubility problems and difficulty in developing an analytical technique when using a set of diverse compounds [3,4]. In order to reduce these issues, it is desirable to keep the number of compounds relatively small and the dose of each to a minimum. The idea of using cassette dosing in ocular pharmacokinetic (PK) studies is a relatively new concept with only a few studies published. One *ex vivo* study of drug partitioning in bovine tissue and a pharmacokinetic study of drug distribution in the rat model using cassette dosing have been successfully completed [5], and another study successfully administered a cassette of five compounds via intravitreal injection to rabbit eyes [6]. Although solid PK data were generated, some variability between the pharmacokinetics of cassette dosing and the pharmacokinetics of individual dosing was noted. However, the results were still regarded as an adequate representation of PK data, and cassette dosing deemed useful for compound screening [6].

Another method of effectively generating ocular PK data without the need for large animal requirements is through the use of an isolated perfused eye system. The isolated perfused eye has

* Corresponding author. Strathclyde Institute of Pharmacy and Biomedical Sciences, University of Strathclyde, 161 Cathedral Street, Glasgow, Scotland G4 0RE, United Kingdom. Tel.: +44 141 548 5947.

E-mail address: andrew.urquhart@strath.ac.uk (A. Urquhart).

been used extensively in a variety of animal models including cat, rat, bull, horse, dog and frog [7–11], and in addition, it has also been used on human eyes [12,13]. More recently, the isolated perfused eye has been utilised in PK studies as an alternative to performing ocular drug distribution studies in live animals. The isolated perfused eye offers several advantages when compared to using an animal during a PK study, including no anaesthetic requirements or concern over animal comfort, control over the physiological environment, reduced animal usage as waste eyes from the food industry can be utilised, controlled drug administration and control of exposure to substances from systemic circulation into the ocular system [14]. Limitations include a lack of neural control of the eye as well as differences between perfusion parameters selected and conditions typically experienced in vivo [15]. In this work, the isolated perfused ovine eye model was used. Ovine eyes have been used previously in isolated perfused eye experiments to investigate the effect of pH on the corneal stroma [16] and carrier mediated uptake of neutral amino acids into the choroid [17]. The relative similarity of the ovine eye size and shape to human eyes and ease of handling make it a useful model in drug distribution studies. Our group has previously demonstrated the use of the isolated perfused ovine eye model through the investigation of fluorescent microparticle distribution in the vitreous and drug distribution using time-of-flight secondary ion mass spectrometry [18,19]. In this study, we present for the first time how the isolated perfused ovine eye can be combined with the method of cassette dosing as a suitable means of generating ocular PK data, reducing both the number of animals required to be utilised during the experimental work and analytical time. We also show that drug lipophilicity plays an important role in the extent of ocular drug distribution following drug administration via an intravitreal injection.

2. Materials and methods

2.1. Isolated ovine eye procedure

Perfusion of the isolated ovine eyes was based on a method detailed previously by Koeberle [20]. Briefly, ovine eyes were collected on ice from a local abattoir, within 1–2 h of slaughter, and warmed to room temperature. One of the long ciliary arteries that typically wrap around the optic nerve was then identified and cannulated in order to supply the perfusion fluid to the eye. Details of the composition of the perfusion fluid administered into the eyes via the ciliary artery are presented in Table 1; all components were purchased from Sigma–Aldrich (Dorset, UK). The eye was placed on the stage of the perfusion system on its side, with the cornea facing outwards, to mimic typical in vivo eye positioning and covered with polyethylene film to prevent dehydration. The cannula was then attached to the filter of the perfusion fluid port, and the perfusion process was initiated at an initial rate of approximately 0.2 ml/minute increased to 1 ml/minute over the course of

30 min. During the perfusion procedure, viability of the isolated perfused ovine eye was determined by monitoring the arterial perfusion pressure, the intraocular pressure (IOP), glucose consumption and lactate dehydrogenase (LDH) activity detailed by Koeberle [20].

2.2. Administration of a beta adrenoreceptor cassette

To investigate the impact of physicochemical properties on drug disposition following intravitreal administration, three different beta adrenoreceptor antagonists were used, atenolol (purity $\geq 98\%$), timolol (purity $\geq 98\%$) and propranolol (purity $\geq 99\%$) – all purchased from Sigma–Aldrich). All three beta adrenoreceptor antagonists were administered to the eye in a cassette. A solution containing atenolol, timolol and propranolol each at a concentration of 5 mg/ml was prepared in deionised water. The solution was then passed through a 0.22 μm syringe filter to remove any particulates. Once the eye had reached maximum perfusion rate and arterial perfusion pressure and intraocular pressure were maintained, the drug cassette was administered into the vitreous. The dose delivered to the eye was 500 μg of each of the three drugs in a total injection volume of 100 μl . The injection was performed using a 1 ml syringe and 23G needle, inserted 5 mm into the vitreous approximately 3–4 mm from the limbus in the posterior direction. Following injection, the needle was drawn very slowly from the eye in order to minimise leakage from the injection site. The perfusion procedure was terminated at five set time points 1, 2, 3, 5 and 7 h post-dosing with the beta adrenoreceptor cassette. For each time point used in the study, five eyes were perfused, dosed and analysed.

2.3. Dissection and ovine ocular tissue preparation

On completion of the perfusion procedure, a 30G needle was inserted into the anterior chamber of the eye, and the aqueous humour was removed. To reduce the risk of cross-tissue contamination, eyes were then frozen in liquid nitrogen before further dissection. The anterior section was removed by creating a small incision into the sclera approximately 3 mm from the edge of the cornea and was then cut away in a circular manner. From this, the lens was lifted away from the iris and ciliary body, and the iris and ciliary body were removed by tweezing the tissue off the sclera. In the posterior section, the eye was placed on its side, and the frozen vitreous was carefully removed using tweezers, ensuring that the retinal tissue did not contaminate the vitreous sample. The retina was then gently lifted away from the head of the optic nerve, and the choroid was also gently lifted away from the sclera. All tissues were then homogenised individually. To the retina, choroid, iris and ciliary body and lens, 1 ml of deionised water was added before homogenisation. Following this, 6 ml of methanol was added to each tissue sample, and samples were ultrasonicated for 2 min. Immediately, the samples were centrifuged for 20 min at a speed of 3000 rpm, and 100 μl was added to 900 μl of deionised water before injection into the UPLC-MS/MS.

2.4. Analysis and quantification of tissue samples

UPLC-MS/MS was performed on a Thermo TSQ Quantum Ultra with HFSI-II heated electrospray ionisation probe (Thermo Scientific). The XCalibur data system was used for system control and also data processing. Analyte separations were performed on an Acquity, BEH UPLC C_{18} column (100 mm length, 2.1 mm internal diameter) with a 1.7 μm particle size. The mobile phase was composed of 0.1% formic acid in HPLC grade water (A) and 0.1% formic acid in methanol (B) at an initial ratio of 95:05 (A:B). A gradient method was selected for compound elution at 500 $\mu\text{l}/\text{min}$, using

Table 1
Composition of perfusion fluid administered to isolated perfused eye.

Chemical	Concentration
Tissue culture medium	1000 ml
Sodium bicarbonate	2.2 g/l
Atropine sulphate	0.005 g/l
EDTA	0.2922 g/l
Penicillin G	100 kU/l
Streptomycin	75.6 kU/l
Gentamycin	0.08 g/l
Insulin bovine	50 U/l
Bovine holo-transferrin	0.0025 g/l
Sodium selenite	2.4 $\mu\text{g}/\text{l}$

the following ratios of mobile phase: 95% A for 0.5 min decreased to 0% using a linear gradient over 0.5 min and held for 1 min, then restored to starting 95% A before the next injection. Samples were analysed in positive mode with selective ion monitoring mode selected to detect the daughter ion of the compounds.

2.5. Analytical method validation

Analytical method validation was performed on all ocular tissues investigated: the aqueous humour, the lens, the iris and ciliary body, the vitreous humour, the retina and the choroid, for all three beta adrenoreceptor antagonists. In order to prepare the samples for the method validation, all tissues were homogenised and spiked with 1 ml of drug compound series and 1 ml of internal standard. The samples were then processed for analysis using the method detailed previously before injection into the UPLC-MS/MS. The method was calibrated and assessed for linearity over the concentration range of 5–100 ng/ml for each individual ocular tissue, using eye tissue from a different animal for each concentration. Weighted linear regression of $1/x^2$ was selected as a suitable method, and acceptable correlation coefficients were obtained for all three drugs in the vitreous, retina, aqueous and lens tissues (>0.97). Weighted linear regression was selected as this method applies focus to data points with lower variance and as a result has less dependence on data associated with high variance, unlike ordinary linear regression, where deviations at higher concentrations tend to have a greater impact on the shape of the calibration curve than deviations at lower concentrations [21,22]. In the choroid, sensitivity was lost at the lowest concentration in the calibration range, and as a result, the calibration curve in this tissue was prepared in the range of 7.5–100 ng/ml. Acceptable accuracy of between 75% and 120% of the ideal value was achieved for all three drugs in the vitreous, retina, aqueous, lens and iris and ciliary body tissues [23]. For the choroid, a slight deviation in accuracy was noted for propranolol (130%). The choroid is a thick melanin rich tissue, and as a result, sample preparation was more challenging and not as clean as the other samples, explaining this deviation. Intraday precision of drug peak area to internal standard peak area was less than 15% and for the interday precision less than 20%.

3. Results and discussion

Three beta adrenoreceptor antagonists (atenolol, timolol and propranolol) were selected for investigation in this study due to their individual physicochemical properties (see Table 2 for values). All three drugs had similar molecular weights (267 a.m.u., 316 a.m.u. and 260 a.m.u., respectively) removing molecular weight influences on drug distribution within the eye [24,25]. All three drugs were basic compounds and had very similar pKa values; since all three drugs were positively charged at physiological pH, pKa would have had little influence on the distribution of each drug. Where a distinct difference did occur in the physicochemical properties of each of the drug compounds was in their partition coefficients. Partition coefficient has been shown to have a large influence on the distribution of drugs within ocular tissues, with hydrophilic molecules thought to distribute and be cleared from the anterior section of the eye and lipophilic molecules thought to distribute and be cleared from the posterior section of the eye [26]. An intravitreal cassette dosing study performed previously in rabbits failed to show clear differences in the impact of partition coefficient on drug distribution within ocular tissues [6]. However, within the drug series selected, all of the drugs were very lipophilic molecules, and this would have accounted for the lack of correlation in drug distribution and partition coefficient. Previous work investigating the impact of beta adrenoreceptor antagonist

lipophilicity on drug distribution following systemic administration in the rat demonstrated that increased tissue accumulation occurred with increasing drug lipophilicity [27]. In this study, atenolol was selected due to its low logP and is the most hydrophilic of the three compounds with a logP of 0.16. Propranolol was selected to be the most lipophilic molecule, with a logP much greater than atenolol at 2.4. Finally, timolol was selected as an intermediate compound with a logP equal to 1.8 sitting between the logP of other two compounds, but leaning more towards the more lipophilic region of the scale.

Following intravitreal drug administration, the corresponding concentration maxima of drug within tissue (C_{Max}) and the time required to reach C_{Max} (T_{Max}) of all three drug molecules in each individual tissue were obtained (see Table 3 for details). The highest concentration of atenolol measured in the vitreous was 2489 $\mu\text{g/g}$ and was recorded in the first hour. Atenolol then appears to move quickly into the iris and ciliary body with C_{Max} recorded to be 5649 $\mu\text{g/g}$ at 2 h post-dosing. Maximal concentrations in the choroid and in the retina were noted simultaneously at 3 h post-dosing and were 2237 and 1014 $\mu\text{g/g}$, respectively, whereas the C_{Max} of the aqueous humour and the lens was seen at 5 h post-dosing and measured to be 426 and 3255 $\mu\text{g/g}$, respectively. In contrast to the data for atenolol, the C_{Max} of timolol was measured in the vitreous humour occurred at the 3 h time point, post-drug administration, however, only at a concentration of 2672 $\mu\text{g/g}$ which is only slightly higher than the concentration of 2664 $\mu\text{g/g}$ seen at 1 h post-dosing. In a similar manner to atenolol, timolol moved quickly into the iris and ciliary body with T_{Max} occurring at 2 h after drug administration, with a corresponding C_{Max} of 7086 $\mu\text{g/g}$. Peak concentrations in the aqueous humour and the lens again occur at 5 h post-dosing, with C_{Max} recorded to be 300 and 4000 $\mu\text{g/g}$, respectively. In this instance, the retina mirrors vitreous humour and not the choroid, with a maximum concentration of 1118 $\mu\text{g/g}$ recorded in the retina at the 3 h time point. The choroid, in contrast to atenolol, reaches a concentration of 3391 $\mu\text{g/g}$ towards the end of the experiment at a T_{Max} of 7 h. With propranolol, again high concentrations were detected in the vitreous in the initial phase of the experiment, with a C_{Max} of 2341 $\mu\text{g/g}$ occurring at 1 h post-administration. In the anterior segment of the eye, the peak aqueous humour concentration occurred at 5 h post-dosing, although concentrations of propranolol in the aqueous humour were generally low throughout the experiment and C_{Max} was determined to be only 108 $\mu\text{g/g}$. As with the other drugs, peak levels of propranolol in the iris and ciliary body occurred at the 2 h time point, and peak levels of propranolol in the lens occurred at 5 h. C_{Max} for both tissues was very similar and was determined to be 5478 $\mu\text{g/g}$ and 5555 $\mu\text{g/g}$, respectively. In similarity to timolol, a peak level in the retina of 1240 $\mu\text{g/g}$ occurred 3 h post-dosing, and in the choroid, a peak level of 4975 $\mu\text{g/g}$ was seen at 7 h after drug administration.

Focusing on the concentration versus time profile for each tissue obtained for each individual drug. For atenolol, there is an initial dip in the vitreous concentration at 2 h, where the drug appears to move quite quickly into the iris and ciliary body (Fig. 1). At this point, it was noted that the drug began to move into the aqueous humour. At 3 h post-dosing, a slight increase in the concentration measured in the vitreous was noted before the concentration again reduced and began to level off at 5 h post-dosing. Corresponding to the vitreous concentration increase, noted at 3 h, there was a dip in the concentration measured in the iris and ciliary body. The iris and ciliary body appeared to act as a reservoir, taking up a high concentration of drug initially before releasing drug back into vitreous when the concentration in the vitreous fell. At the three hour time point, the vitreous supplies the posterior tissues and increases in choroid and retina concentrations also occurred. The concentration time profiles of the choroid and the

Table 2
Physiochemical properties of the drugs within the drug cassette.

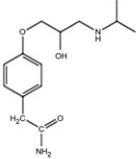
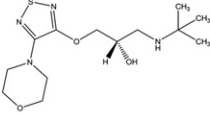
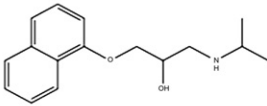
Beta adrenoreceptor antagonist	pKa	LogP	Structure
Atenolol	9.5	0.16	
Timolol	9.2	1.8	
Propranolol	9.3	2.4	

Table 3
 C_{Max} and T_{Max} obtained for atenolol, timolol and propranolol in each individual ocular tissue.

Tissue	C_{Max} (ng/g)	T_{Max} (h)
<i>Atenolol</i>		
Aqueous	426.32	5
Iris and ciliary body	5648.98	2
Lens	3254.83	5
Vitreous	2488.78	1
Retina	1014.08	3
Choroid	2237.10	3
<i>Timolol</i>		
Aqueous	299.86	5
Iris and ciliary body	7086.28	2
Lens	3999.93	5
Vitreous	2672.32	3
Retina	1117.88	3
Choroid	3391.22	7
<i>Propranolol</i>		
Aqueous	59.48	1
Iris and ciliary body	5477.54	2
Lens	5555.18	5
Vitreous	2341.12	1
Retina	1239.80	3
Choroid	4975.08	7

retina appear to mirror each other, suggesting steady state exchange of drug between the two tissues. Another larger dip in the iris and ciliary body concentration occurred after 5 h, where atenolol moved out of the iris and ciliary body and into the other anterior tissues, the aqueous humour and the lens.

Focusing on the concentration versus time profiles generated for timolol (Fig. 2), a similar pattern of drug distribution to atenolol was seen, with differences in concentration profile occurring in the retina and in the choroid. Initially, timolol moved quickly out from the vitreous humour and into the iris and ciliary body within the first 2 h of the experiment. Differing from atenolol, at the 2 h time point, we had also seen rapid movement of timolol from the vitreous humour and into the retina, with concentrations in the retina rising steadily over the first 3 h as drug began to move in the posterior direction. At 3 h post-administration, timolol appeared to

move back from the iris and ciliary body into the vitreous which, at the point, feeds the posterior retina and choroid tissues. Increases in drug movement into the anterior chamber occurred again at 5 h post-dosing, with increases in aqueous and lens concentrations in response to a corresponding dip in the concentration achieved in the iris and ciliary body. Finally, towards the end of the experiment, drug began to accumulate in the choroid, which facilitated rising concentrations in the retina.

Propranolol moved in the anterior direction from the vitreous to the iris and ciliary body in the first 2 h, but again the drug also moved in the posterior direction, and the levels in the retina began to rise too (see Fig. 3). Propranolol was then dislodged from the iris and ciliary body at 3 h post-administration and moved back into the vitreous tissue, with simultaneous increases in concentrations detected in the retina and in the choroid. This effect was seen across all three drugs, and it is also possible that the increased vitreous concentrations were not only due to drug dislodgement from the iris and ciliary body but from drug movement through the lens into the vitreous humour. Tan et al. have noted from the ocular fluorophotometry in live rabbit eyes that intravitreally injected sodium fluorescein penetrated the lens at 2 h after dosing, but the substance did not continue a forward diffusion into the anterior chamber but unloaded the absorbed fluorescein back into the vitreous humour 3 h later [28]. This coincides with the study by Stepanova and colleagues, who showed that when fluorescein was initially placed in the central section of the lens, it rapidly moved towards the posterior pole of the lens and out into the vitreous humour, with no fluorescein shown to move in the anterior direction [29]. In this case, it was postulated that fluorescein movement was caused by a vectorial fluid flow in the lens that opposes diffusion, most likely mediated by the transport system present in the lens epithelium. After 5 h, another fall in the iris and ciliary body concentration occurred, corresponding to an increase in the concentration of propranolol in the lens. At the end of the experiment, as with timolol, a spike in the concentration of propranolol detected in the choroid occurred and fed the retina with a rich supply of drug. However, the concentration of propranolol bound to the choroid was much greater than the concentration of timolol measured.

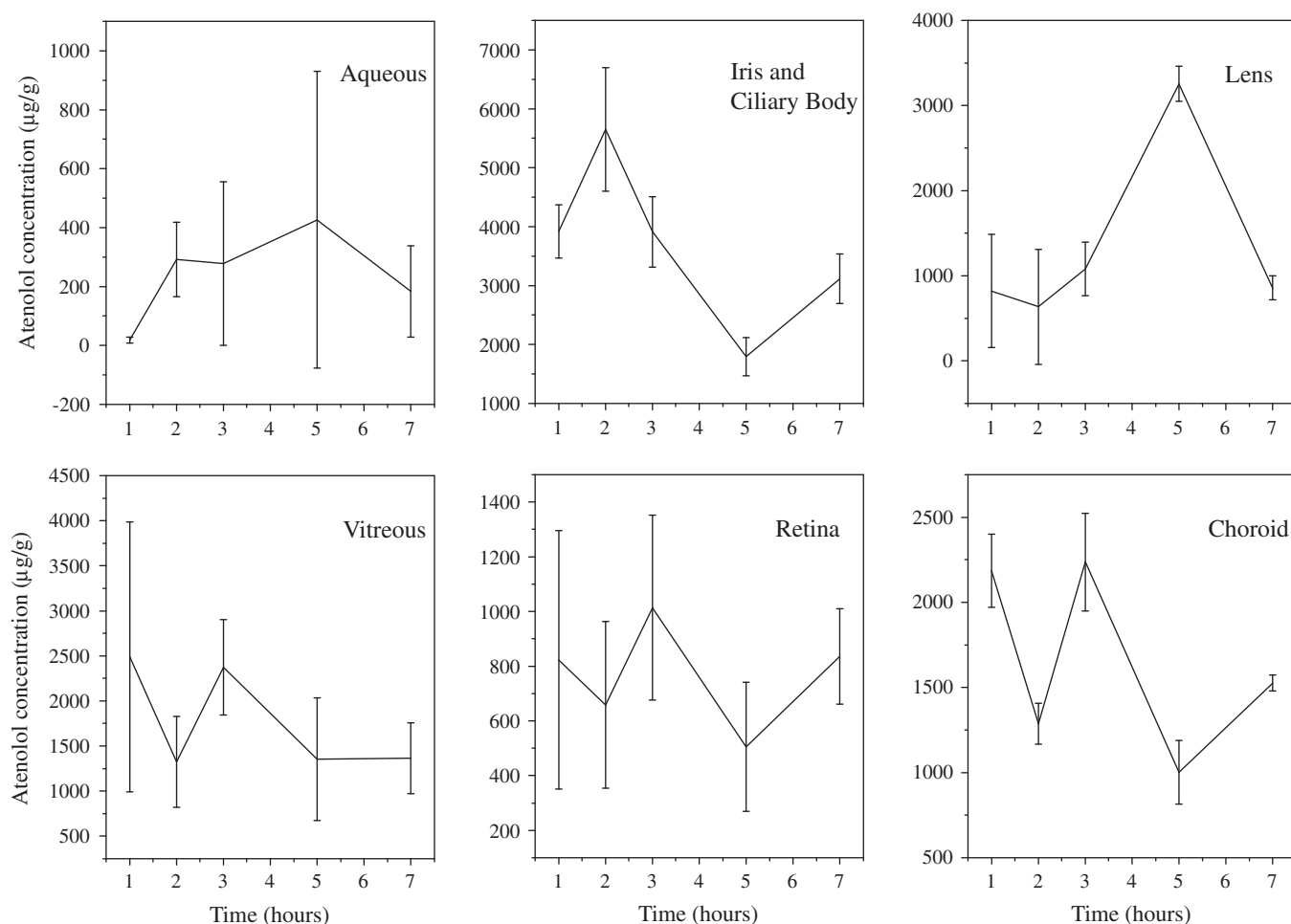


Fig. 1. Mean concentration ($n = 5$) versus time profile obtained for atenolol in each individual ocular tissue. Error bars show standard deviation from the mean.

Directly comparing the C_{Max} achieved for each of the three beta adrenoreceptor antagonists used shows key differences in drug distribution patterns (see Fig. 4). In the anterior segment of the eye, differences in C_{Max} occurred in all three tissues investigated, the aqueous humour, the lens and the iris and ciliary body. In the aqueous humour, the highest C_{Max} was achieved by the most hydrophilic molecule, atenolol, followed by a reduction in C_{Max} according to decreasing hydrophilicity, with timolol higher than propranolol. More hydrophilic compounds have been shown to penetrate and have greater diffusivity within the water based aqueous humour than more lipophilic drug compounds [26]. Therefore, an increase in the aqueous humour C_{Max} of the three beta blocking compounds with decreasing logP was due to an increase in the ease of drug diffusion into the aqueous humour because of drug hydrophilicity. More hydrophilic compounds are also subject to removal through the aqueous clearance system and will migrate from the vitreous into the anterior section of the eye before removal [30,31]. Therefore, a higher concentration of the more hydrophilic drug, atenolol, moved in the anterior direction than the other two more lipophilic drugs. In contrast to a previous study, where T_{Max} in the aqueous humour was shown to increase with increasing logP, no significant difference between the compounds was recorded for T_{Max} , with T_{Max} determined to be 5 h post-dosing for atenolol and timolol, and 1 h for propranolol [26]. The difference in trends in T_{Max} could be related to the molecular size of the compounds used in the previously study, as the logP of the compounds corresponded to a progressive increase in molecular size [23], whereas in this study, no such relationship

between size and partition coefficient existed. Significant differences in C_{Max} were noted in the iris and ciliary body with timolol, showing the greatest binding to this tissue followed by atenolol and then closely followed by propranolol, with a difference between the two of 200 µg/g. For the lens, a progressive increase in penetration into this tissue was seen with increasing drug lipophilicity. Movement of compounds within the lens has previously been investigated using fluorescein as a drug marker [29,32]. In the rabbit eye, it was demonstrated that fluorescein penetrated into the lens at both the anterior side and the posterior side, with little resistance created by the lens capsule. Resistance to fluorescein entry into the lens was, however, caused by the lens epithelium. For this reason, compounds with a higher partition coefficient will more readily penetrate the epithelial barrier than more hydrophilic drugs, explaining the rank order in drug penetration into the lens tissue with increasing lipophilicity [32].

In the posterior segment, and at the site of initial drug administration, little difference in the C_{Max} measured in the vitreous humour across the drug series was noted. The C_{Max} of timolol appeared to be the greatest, but the difference was small with a large variance. A difference in T_{Max} also occurred across the tissues, with the T_{Max} of atenolol and propranolol recorded at 1 h and the T_{Max} of timolol determined to be 3 h. The vitreous has been shown to experience an initial drug diffusion stage over the first hour following administration, followed by a gradual drug elimination phase, explaining the T_{Max} of one hour obtained for atenolol and propranolol [26,33]. As discussed previously, all three drugs also show an increase in measured drug levels at three hours, due to drug

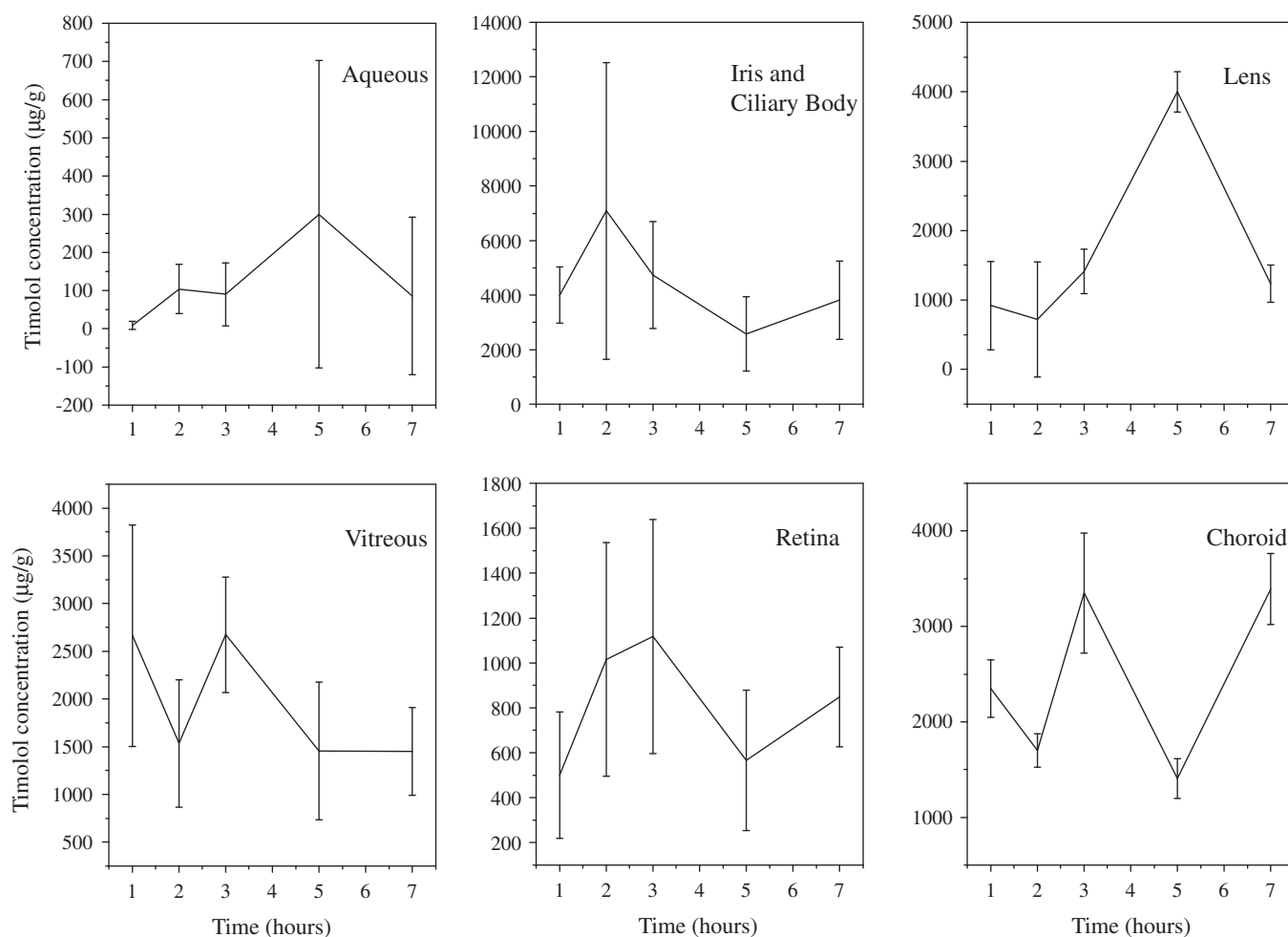


Fig. 2. Mean concentration ($n = 5$) versus time profile obtained for timolol in each individual ocular tissue. Error bars show standard deviation from the mean.

displacement from the iris and ciliary body and re-equilibrating through the lens back into the vitreous. As a result, for all three drugs, similar drug levels were obtained at both one hour and three hours post-dosing. For timolol, the level obtained at three hours was just slightly greater than the level obtained at one hour, accounting for the apparent difference in T_{Max} compared to the other drugs in the series. In the remaining posterior tissues, the retina and the choroid, a pattern in the extent of drug movement was seen. In the retina, a stepwise increase was noted with increasing lipophilicity, with atenolol having the lowest C_{Max} , followed by timolol and then by propranolol with the greatest C_{Max} . The retina mirrored the choroid with a progressive increase in C_{Max} with increasing lipophilicity. The increase in choroid levels with increasing lipophilicity is in keeping with previous observations from the rat eye following a trans-scleral injection of a beta blocker drug series [5]. However, in this case, the choroid did not mirror the retina as retinal levels decreased with increasing lipophilicity. The lack of correlation could be explained by the difference in route of administration, as following trans-scleral injection, the beta blocker drug mix would reach the choroid before penetrating into the vitreous. The more lipophilic drugs would have bound to the choroidal melanin, and as a result, less drug would be free to move into the vitreous. Lipophilic drugs are subject to retinal clearance and will migrate towards the posterior pole before subsequent elimination [20,26]. As a result, a progressive increase in drug levels in the posterior eye with increasing lipophilicity is seen, as more hydrophilic drugs tend to move towards the anterior section

of the eye. T_{Max} differed also in the choroid, with C_{Max} occurring much earlier for atenolol at 3 h post-dosing, whereas drug accumulation on the choroid with time occurred for timolol and propranolol, with C_{Max} determined at 7 h post-dosing. The delay in reaching C_{Max} was probably caused by progressive drug accumulation on the melanin contained in the choroid over the course of the perfusion. Beta adrenoreceptor antagonists have previously been shown to bind to melanin of the choroid/RPE (retinal pigmented epithelium) with a high percentage of the available drug accumulating on the melanin [34]. It has been reported that all drugs known to bind to melanin are basic or have some element of basicity in their structure, and in addition to this, all drugs were known to have a positive logP and therefore a degree of lipophilicity [35]. All three drugs used in this study were basic compounds, with varying levels of lipophilicity. It is interesting that the extent of binding to the choroid tissue increased with increasing drug lipophilicity. This differs from the results obtained in the iris and ciliary body, where a stepwise increase in drug tissue binding with increasing lipophilicity was not demonstrated and timolol had the highest C_{Max} out of the three drugs investigated. This difference may be influenced by the clearance mechanisms operating within the eye, as propranolol is very lipophilic and subject to retinal clearance, less propranolol would be available in the anterior section of the eye than the less lipophilic timolol, accounting for the reduced levels experienced on the iris and ciliary body. In addition, although a higher concentration of atenolol would have migrated towards the anterior eye, the more hydrophilic nature of atenolol

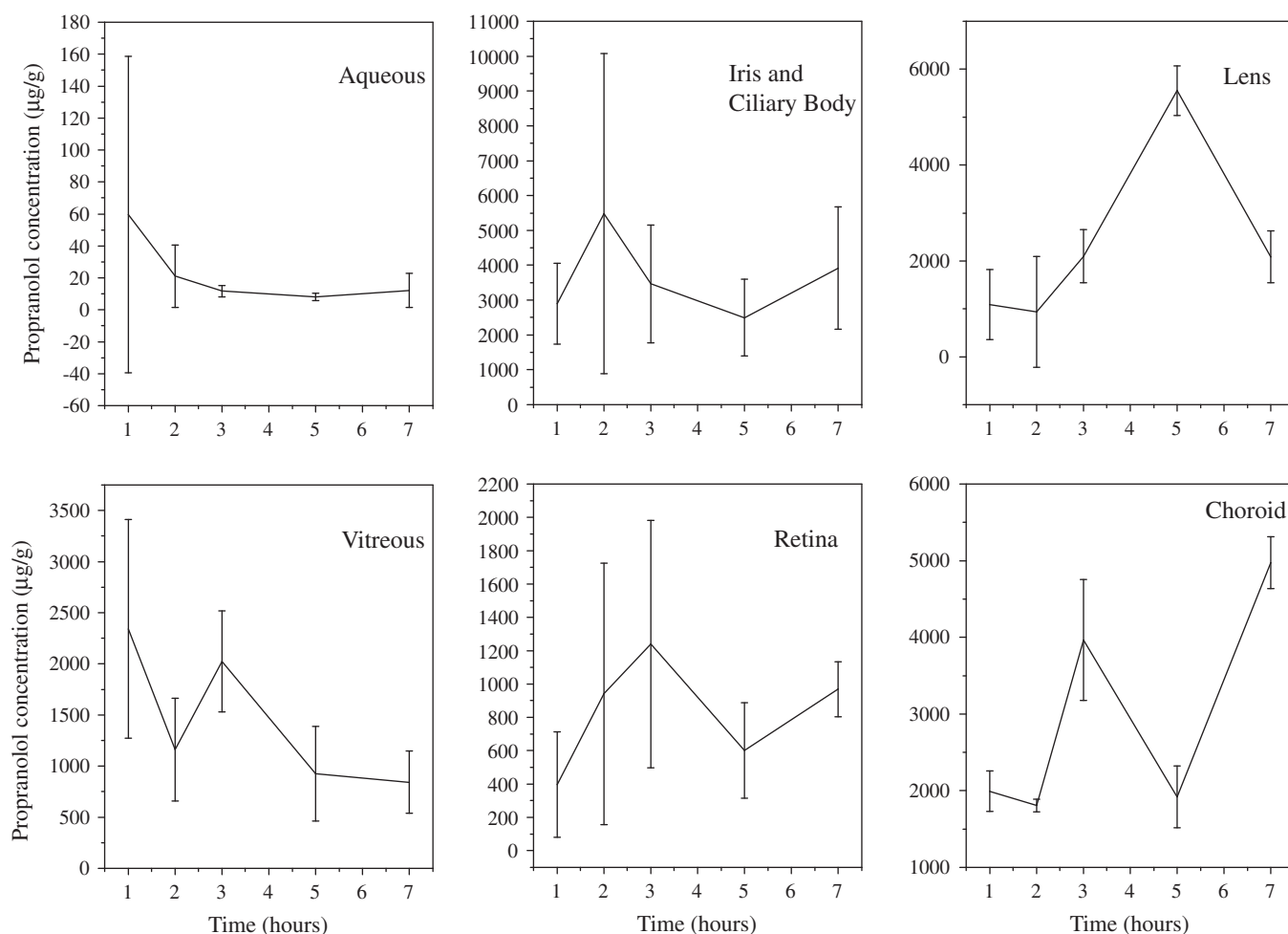


Fig. 3. Mean concentration ($n = 5$) versus time profile obtained for propranolol in each individual ocular tissue. Error bars show standard deviation from the mean.

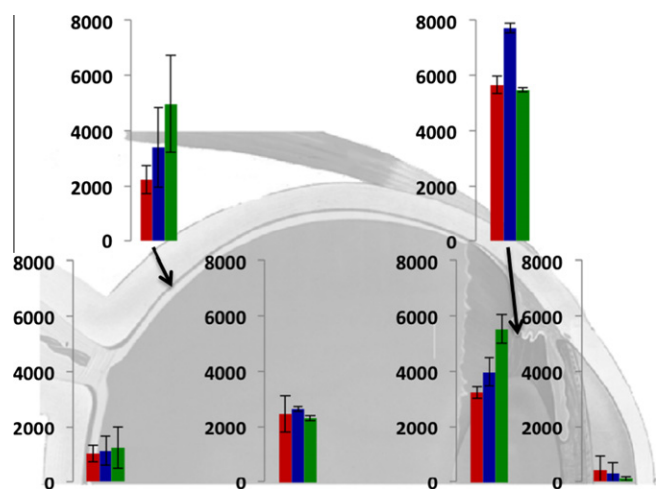


Fig. 4. C_{max} (y axis in µg/g) obtained for atenolol (red column), timolol (blue column) and propranolol (green column) in each ocular tissue ($n = 5$) shown at the position of the tissue within the eye. Error bars show standard deviation from the mean. Moving from left to right, retina, choroid, vitreous, lens, iris and ciliary body and finally aqueous humour. (For interpretation of the references to colour in this figure legend, the reader is referred to the web version of this article.)

would have reduced the extent of atenolol binding to the melanin of the iris and ciliary body. Although the iris and ciliary body and the retina are both melanin rich tissues, the melanin structure

within these tissues is slightly different. The uveal tract is known to contain two types of melanin, pheomelanin and eumelanin, whereas the choroid is thought to contain mainly eumelanin. Pheomelanin is a lighter coloured pigment, and the content of pheomelanin varies between eyes with a higher ratio of pheomelanin/eumelanin existing in lighter coloured eyes [36]. The pheomelanin content of the iris, choroid and RPE has been previously shown to be low for all three tissues; however, distinct differences in content existed across the tissue range with 1% pheomelanin content in the iris, 0.1–0.5% in the RPE and a negligible amount in the choroid [37]. The basic melanin composition between the tissues also differs, with differences in the elemental composition of melanin contained in the iris, the choroid and the RPE previously demonstrated [38]. In the human eye, differences in eumelanin content of the melanocytes of the iris and the melanocytes of the choroid were apparent. Although not statistically significant, eumelanin content in the choroidal melanocytes was shown to be greater in the melanocytes of the choroid compared to the melanocytes of the iris [39]. In the bovine eye, differences in the amino acid content of melanin containing tissues were apparent, with amino acid content higher in the choroid than in the iris and the RPE [37]. It is likely that the structural differences in the varying types of melanin played a role in the differences in the extent drug accumulation in the choroid; however, investigations directly comparing drug binding to the different melanin binding tissues of the eye are limited. Further work is still required on drug accumulation on melanin isolated from the choroid and the iris of the ovine eye in

order to determine the importance of both melanin biochemistry and melanin composition within ocular tissues.

In addition to melanin binding phenomena, drug transporter systems are thought to have a key role in the transfer of materials at the RPE and therefore drug movement from the vitreous to the retina and the choroid [40,41]. Various drug transporter systems have previously been shown to play a role in drug distribution in the posterior eye, including P-glycoprotein, organic cation transporters and organic anion transporters [42–44]. Although the involvement of drug transport systems in the extent of drug penetration of the drug series into the retina and the choroid was out with the scope of this study and remains unclear, the impact of drug lipophilicity on drug levels with the retina and choroid has been demonstrated. The potential involvement of drug transport systems cannot be disregarded and therefore should be taken into consideration when interpreting the results.

This work has demonstrated that cassette dosing using the isolated perfused ovine eye is a suitable means of carrying out drug distribution studies, significantly reducing both the number of animals utilised during the experimental work and analytical time. The results reported here have clearly shown that drug lipophilicity plays an important role in the extent of ocular drug distribution following drug administration via an intravitreal injection. Drugs with greater lipophilicity will penetrate to the posterior eye, residing in the retina and the choroid at greater levels than those seen for more hydrophilic drugs. This will impact on the drug candidate selection process for the treatment of posterior eye diseases such as age-related macular degeneration and diabetic retinopathy, where the desire is to penetrate to the back of the eye at desirable drug concentrations. Further work is still required in order to understand the impact both drug transport mechanisms and melanin biochemistry/tissue composition have on drug distribution within the choroid and the iris and ciliary body.

Acknowledgement

JM acknowledges AstraZeneca and University of Strathclyde for the studentship. We thank Anthony Atkinson from AstraZeneca R&D, Charnwood for assistance with UPLC-MS/MS measurements.

References

- [1] B.L. Ackermann, Ackermann, Results from a bench marking survey on cassette dosing practices in the pharmaceutical industry, *Journal of the American Society for Mass Spectrometry* 15 (2004) 1374–1377.
- [2] P. Manitspitskul, R.E. White, Whatever happened to cassette-dosing pharmacokinetics?, *Drug Discovery Today* 9 (2004) 652–658.
- [3] R.E. White, P. Manitspitskul, Pharmacokinetic theory of cassette dosing in drug discovery screening, *Drug Metabolism and Disposition* 29 (2001) 957–966.
- [4] L.W. Frick, K.K. Adkison, K.J. Wells-Knecht, P. Woollard, D.M. Higton, Cassette dosing: rapid in vivo assessment of pharmacokinetics, *Pharmaceutical Science & Technology Today* 1 (1998) 12–18.
- [5] R.S. Kadam, U.B. Kompella, Influence of lipophilicity on drug partitioning into sclera, choroid-retinal pigment epithelium, retina, trabecular meshwork, and optic nerve, *The Journal of Pharmacology and Experimental Therapeutics* 332 (2010) 1107–1120.
- [6] J.W. Proksch, K.W. Ward, Cassette dosing pharmacokinetic studies for evaluation of ophthalmic drugs for posterior ocular diseases, *Journal of Pharmaceutical Sciences* 97 (2007) 3411–3421.
- [7] A.H. Friedman, A.L. Marchese, The isolated perfused frog eye: a useful preparation for the investigation of drug effects on retinal function, *Journal of Pharmacological Methods* 5 (1981) 215–234.
- [8] H. Ripps, L. Mehafeff, I.M. Siegel, G. Niemeyer, Vincristine-induced changes in the retina of the isolated arterially-perfused cat eye, *Experimental Eye Research* 48 (1989) 771–790.
- [9] E.-N. Su, D.-Y. Yu, V.A. Alder, P.K. Yu, S.J. Cringle, Altered vasoactivity in the early diabetic eye: measured in the isolated perfused rat eye, *Experimental Eye Research* 61 (1995) 699–711.
- [10] M. Wiederholt, S. Bielka, F. Schweig, E. Lütjen-Drecoll, A. Lepple-Wienhues, Regulation of outflow rate and resistance in the perfused anterior segment of the bovine eye, *Experimental Eye Research* 61 (1995) 223–234.
- [11] I.A. Shiels, S.D. Sanderson, S.M. Taylor, Arterially perfused eye model of uveitis, *Australian Veterinary Journal* 2 (1999) 100–104.
- [12] B.G. Dijkstra, A. Schneemann, P.F. Hoyng, Flow after prostaglandin E1 is mediated by receptor-coupled adenylyl cyclase in human anterior segments, *Investigative Ophthalmology and Visual Science* 40 (1999) 2622–2626.
- [13] J. Gottanka, D. Chan, M. Eichhorn, E. Lutjen-Drecoll, C.R. Ethier, Effects of TGF- β 2 in perfused human eyes, *Investigative Ophthalmology and Visual Science* 45 (2004) 153–158.
- [14] G. Niemeyer, Retinal research using the perfused mammalian eye, *Progress in Retinal and Eye Research* 20 (2001) 289–318.
- [15] D.-Y. Yu, E.-N. Su, S.J. Cringle, P.K. Yu, Isolated preparations of ocular vasculature and their applications in ophthalmic research, *Progress in Retinal and Eye Research* 22 (2003) 135–169.
- [16] M.J. Doughty, Use of a corneal stroma perfusion technique and transmission electron microscopy to assess ultrastructural changes associated with exposure to slightly acidic pH 5.75 solutions, *Current Eye Research* 33 (2008) 45–57.
- [17] J.E. Preston, M.B. Segal, G.J. Walley, B.V. Zlokovic, Neutral amino acid uptake by the isolated perfused sheep choroid plexus, *Journal of Physiology* 408 (1989) 31–43.
- [18] L.E. Tan, A model of ageing vitreous: implications for drug delivery, in: SIPBS, University of Strathclyde, Glasgow, 2010, p. 272.
- [19] J. Mains, C. Wilson, A. Urquhart, ToF-SIMS analysis of ocular tissues reveals biochemical differentiation and drug distribution, *European Journal of Pharmaceutics and Biopharmaceutics* 79 (2011) 328–333.
- [20] M. Koeberle, Investigation of factors involved in the disposition and pharmacokinetics of memantine in the isolated bovine eye, University of Strathclyde, Glasgow, 2002.
- [21] N.V. Nagaraja, J.K. Paliwal, R.C. Gupta, Choosing the calibration model in assay validation, *Journal of Pharmaceutical and Biomedical Analysis* 20 (1999) 433–438.
- [22] T. Singtoroj, J. Tarning, A. Annerberg, M. Ashton, Y. Bergqvist, N.J. White, N. Lindegardh, N.P.J. Day, A new approach to evaluate regression models during validation of bioanalytical assays, *Journal of Pharmaceutical and Biomedical Analysis* 41 (2006) 219–227.
- [23] H. Hendrickson, E. Laurenana, M. Owens, Quantitative determination of total methamphetamine and active metabolites in rat tissue by liquid chromatography with tandem mass spectrometric detection, *AAPS Journal* 8 (2006) 709–717.
- [24] I. Fatt, Flow and diffusion in the vitreous body of the eye, *Bulletin of Mathematical Biology* 37 (1975) 85–90.
- [25] J. Kathawate, S. Acharya, Computational modeling of intravitreal drug delivery in the vitreous chamber with different vitreous substitutes, *International Journal of Heat and Mass Transfer* 51 (2008) 5598–5609.
- [26] H. Atluri, A.K. Mitra, Disposition of short-chain aliphatic alcohols in rabbit vitreous by ocular microdialysis, *Experimental Eye Research* 76 (2003) 315–320.
- [27] T. Rodgers, D. Leahy, M. Rowland, Tissue distribution of basic drugs: Accounting for enantiomeric, compound and regional differences amongst b-blocking drugs in rat, *Journal of Pharmaceutical Sciences* 94 (2005) 1237–1248.
- [28] L.E. Tan, W. Orilla, P. Hughes, S.T. S. J. Burke, C.G. Wilson, Effects of vitreous liquefaction on intravitreal distribution of sodium fluorescein, fluorescence dextran and fluorescent microparticles, *Investigative Ophthalmology and Visual Science* 52 (2011) 1111–1118.
- [29] L.V. Stepanova, I.Y. Marchenko, G.M. Synchev, Direction of fluid transport in the lens, *Bulletin of Experimental Biology and Medicine* 139 (2005) 50–51.
- [30] M. Araie, D.M. Maurice, The loss of fluorescein, fluorescein glucuronide and fluorescein isothiocyanate dextran from the vitreous by the anterior and retinal pathways, *Experimental Eye Research* 52 (1991) 27–39.
- [31] P.M. Beer, S.J. Bakri, R.J. Singh, W. Liu, G.B. Peters, M. Miller, Intraocular concentration and pharmacokinetics of triamcinolone acetonide after a single intravitreal injection, *Ophthalmology* 110 (2003) 681–686.
- [32] R.J. Kaiser, D.M. Maurice, The diffusion of fluorescein in the lens, *Experimental Eye Research* 3 (1964) 156–165.
- [33] T. Hu, Q. Le, Z. Wu, W. Wu, Determination of doxorubicin in rabbit ocular tissues and pharmacokinetics after intravitreal injection of a single dose of doxorubicin-loaded poly-[beta]-hydroxybutyrate microspheres, *Journal of Pharmaceutical and Biomedical Analysis* 43 (2007) 263–269.
- [34] L. Pitkanen, V. Ranta, H. Moilanen, A. Urtti, Binding of betaxolol, metoprolol and oligonucleotides to synthetic and bovine ocular melanin, and prediction of drug binding to melanin in human choroid-retinal pigment epithelium, *Pharmaceutical Research* 24 (2007) 2063–2070.
- [35] B. Leblanc, S. Jezequel, T. Davies, G. Hanton, C. Taradach, Binding of drugs to eye melanin is not predictive of ocular toxicity, *Regulatory Toxicology and Pharmacology* 28 (1998) 124–132.
- [36] G. Protá, D.-N. Hu, M.R. Vincensi, S.A. McCormick, A. Napolitano, Characterization of melanins in human irides and cultured uveal melanocytes from eyes of different colors, *Experimental Eye Research* 67 (1998) 293–299.
- [37] Y. Liu, L. Hong, K. Wakamatsu, S. Ito, B.B. Adhyaru, C. Cheng, C. Bowers, J.D. Simon, Comparisons of the structural and chemical properties of melanosomes isolated from retinal pigment epithelium, iris and choroid of newborn and mature bovine eyes, *Photochemistry and Photobiology* 81 (2005) 510–516.

- [38] T.P. Dryja, M. O-Neil-Dryja, D.M. Albert, Elemental analysis of melanins from bovine hair, iris, choroid and retinal pigment epithelium, *Investigative Ophthalmology and Visual Science* 18 (1979) 231–236.
- [39] K. Wakamatsu, D. Hu, S.A. McCormick, S. Ito, Characterisation of melanin in human iridal and choroidal melanocytes from eyes with various colored irides, *Pigment Cell Melanoma Research* 21 (2007) 97–105.
- [40] M.E. Smith, M.C. Kincaid, C.E. West, *Basic Science, Refraction, and Pathology. The Requisites in Ophthalmology*, first ed., Mosby-Year Book Inc., 1999.
- [41] C.G. Wilson, E.M. Semenera, P.M. Hughes, O. Olejnik, Eye structure and physiological function, in: E. Touitou, B.W. Barry (Eds.), *Enhancement in Drug Delivery*, Taylor and Francis Group, LLC, 2007, pp. 473–486.
- [42] Y. Han, D.H. Sweet, D. Hu, J.B. Pritchard, Characterization of a novel cationic drug transporter in human retinal pigment epithelial cells, *Journal of Pharmacology and Experimental Therapeutics* 296 (2001) 450–457.
- [43] K. Hosoya, Y. Ohshima, K. Katayama, M. Tomi, Use of microdialysis to evaluate efflux transport of organic anions across the blood-retinal barrier, *AAPS Journal* (2003) 583.
- [44] H. Steuer, A. Jaworski, B. Elger, M. Kaussmann, J. Keldenich, H. Schneider, D. Stoll, B. Schlosshauer, Functional characterization and comparison of the outer blood-retinal barrier, *Investigative Ophthalmology and Visual Science* 46 (2005) 1047–1053.